



HAL
open science

1.65 μm Er:YAG hybrid fibered/bulk emitter for CH₄ differential absorption lidar

Dimitri Edouart, Fabien Gibert, Claire Cénac

► **To cite this version:**

Dimitri Edouart, Fabien Gibert, Claire Cénac. 1.65 μm Er:YAG hybrid fibered/bulk emitter for CH₄ differential absorption lidar. 31st International Laser Radar Conference, Jun 2024, Landshut, Germany. hal-04727517

HAL Id: hal-04727517

<https://hal.science/hal-04727517v1>

Submitted on 11 Oct 2024

HAL is a multi-disciplinary open access archive for the deposit and dissemination of scientific research documents, whether they are published or not. The documents may come from teaching and research institutions in France or abroad, or from public or private research centers.

L'archive ouverte pluridisciplinaire **HAL**, est destinée au dépôt et à la diffusion de documents scientifiques de niveau recherche, publiés ou non, émanant des établissements d'enseignement et de recherche français ou étrangers, des laboratoires publics ou privés.

1.65 μm Er:YAG hybrid fibered/bulk emitter for CH₄ differential absorption lidar

Dimitri Edouart, Fabien Gibert and Claire Cénac

Laboratoire de Météorologie Dynamique (LMD/IPSL), École polytechnique, Institut polytechnique de Paris, Sorbonne Université, École normale supérieure, PSL Research University, CNRS, École des Ponts, Palaiseau, France, E-mail:gibert@lmd.polytechnique.

Abstract: A new Differential Absorption Lidar (DIAL) for atmospheric methane (CH₄) profile measurement is under development at LMD. The lidar emitter is a new hybrid fibered/bulk Er:YAG laser. Two Erbium doped fiber lasers at 1532 nm are used to pump an Er:YAG rod in a ring cavity. The pulsed laser is sequentially injection-seeded by 2 fiber coupled CW Distributed Feedback (DFB) laser diodes On and Off respectively in the center of the methane line triplet at 1645.55 nm and out of at 1645.3 nm. It delivers dual On/Off 8 mJ/ 300 ns pulses at a repetition frequency of 1 kHz but other configuration can also be chosen. In this paper, we will present the objectives of this work, describe the experimental set-up and the laser performances with respect to power efficiency, beam quality, spectral purity and stability.

1. Introduction

Methane (CH₄) is the second anthropogenic greenhouse gas (GHG) in the atmosphere that contributes to the global warming after CO₂. If the methane emissions have a unique sink by OH oxidation, the various different sources, both anthropogenic (around 2/3) and natural, make complex the understanding of its atmospheric concentration. On the anthropogenic side (mainly gas exploitation and burning) it is fundamental to have a tool to verify inventories at different scales (from local methanizer to megacity) and prevent production network leakage in the atmosphere. As for surface-atmosphere exchanges of CO₂, it is fundamental to study at different scales the spatial pattern and magnitude of the natural CH₄ sources (biogenic anaerobic degradation of organic matter in wetlands, landfill and waste, livestock, rice cultivation, termite, geological sources) and to understand their evolution with the global warming.

Lidar has an important role to play in such topic as it can make: (i) a 3D mapping of CH₄ concentration in anthropogenic plumes, (ii) vertical profiles to study transport processes in the atmosphere, (iii) even measure direct flux and (iv) provide CH₄ Earth global measurements from a space platform as it will be for MERLIN CH₄ integrated path differential absorption lidar CNES/DLR ongoing mission [1].

The usual way to obtain a laser emission at 1.645 μm for lidar application is to use frequency conversion with a pulsed Nd:YAG laser and an OPO (optical parametric oscillation) seeded cavity [2]. Er:YAG laser has also been used but low emission cross-section, limited erbium excited level life-time reduced the performances of such architecture [3]. In addition the line multiplet of CH₄ centered at 1645.55 nm is located on the side of Er:YAG emission gain band. To obtain dual laser emission for CH₄ DIAL at 1645 nm, Wang et al (2013) used several intra-cavity etalons [4] but the performances of their laser was judged as unrealistic by Aubourg et al. (2014) [5].

In this framework, we then re-visit hybrid fibered/bulk Er:YAG emitter dedicated for CH₄ differential absorption lidar (DIAL). In this paper, we will describe the experimental set-up and present some results showing the laser performances.

2. Experimental set-up

The laser set-up is shown in Fig. 1. A ring cavity contains a 8 cm long 0.25 % doped Er:YAG crystal rod and an acousto-optic modulator (AOM) to generate laser pulses. The transmission of the output coupler is 20 %. Two 30-W linearly polarized Erbium doped fiber lasers (IPG Photonics - model ELR-30-1532-LP) are combined using a polarization beam splitter (PBS) to end pump the Er:YAG crystal. Another PBS inside the laser cavity is used to

obtain a linear polarization of the pulsed laser. The laser cavity is alternatively injection-seeded by two CW fiber coupled distributed feedback (DFB) laser diode using a fiber switch (SWT). The seeders are coupled into the laser cavity through the AOM first diffraction order. A boost optical amplifier (BOA) is used to amplify the seeders power. One DFB wavelength is positioned in the center of a methane triplet line at 1645.55 nm and the other one out of at 1645.3 nm. The wavelengths are monitored using a wave-meter with 10 MHz precision and 30 MHz accuracy. In a second step, a frequency reference system with a CH₄ absorption cell will be used. Both wavelengths are held in resonance inside the laser cavity using a double phase servo loop [6]. The servo loop is based on a Pound Drever Hall (PDH) scheme with a phase modulation at 150 MHz applied by an electro-optic modulator (EOM). As shown in Fig. 2, the laser is mounted on a dedicated 40 cm long invar plate. The crystal and the AOM are conductively cooled using Peltier components that are thermally isolated from the plate. The heat is dissipated below the plate thanks to cooling fans. The invar plate has been chosen to limit the frequency drift of the laser cavity.

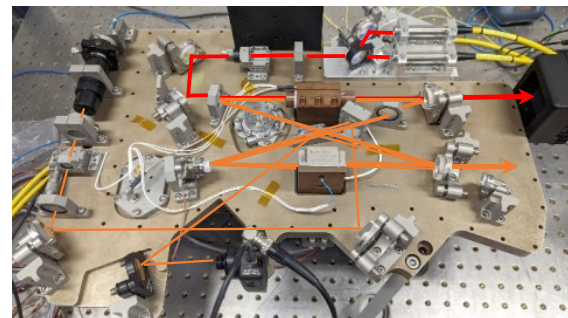


Figure 2. Laser cavity photograph

3. Laser performances

Figure 3 displays the output pulse energy versus the pump power at 2 kHz pulse repetition rate (PRF). The waist radius in Er:YAG rod was estimated to be around 550 μm with output laser beam divergence measurement. At 60 W pump power we obtain 11 W at 1645 nm (17% optical to optical efficiency) and 8.5 W at 1645.55 nm. Such performances are similar to Shen et al. (2019) although their laser architecture was different and no dual wavelength operation of their laser was demonstrated [7].

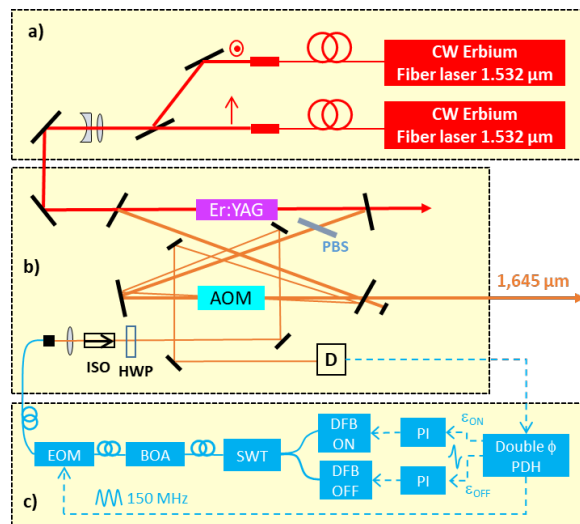


Figure 1. Laser experimental set-up. a) pump fiber lasers @1532 nm, b) laser cavity @1645 nm, c) ON and OFF seeders. AOM :Acousto-Optic Modulator, HWP : Half Wave Plate, PBS: Polarisation Beam Splitter, DFB: Distributed Feedback laser EOM: Electro-Optic Modulator, BOA: Booster Optical Amplifier, SWT: Switch, D: detector, PI: Proportional Integral, PDH: Pound Drever Hall.

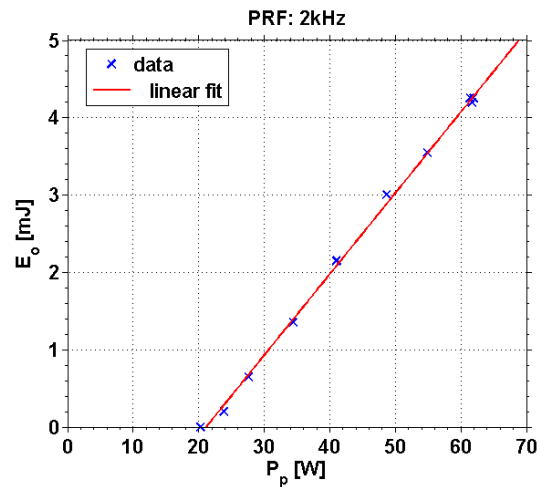


Figure 3. Output pulse energy vs. pump power at 2kHz pulse repetition rate

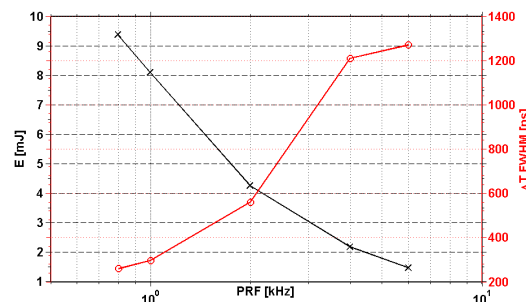


Figure 4. Output pulse energy and pulse duration (Full Width at Half Maximum) vs. the pulse repetition frequency.

The output pulse energy and the full width at half maximum pulse duration as a function of the pulse repetition frequency (PRF) is displayed in Fig. 4. When the pulse repetition frequency increases, the output power slightly increases but the pulse duration is too large that limits the lidar range resolution (1 μ s means 150 m range resolution). At 1 kHz, the pulse energy reaches 8 mJ and the pulse duration is 300 ns. This set point seems to be a good choice for a direct detection DIAL measurement.

When the laser cavity is seeded by the ON and OFF wavelengths, the output pulse energies are not equal because Erbium emission cross section is lower at 1645.55 nm than at 1645.3 nm. The resulting energy differences can be seen in the top graph of the Fig. 5 showing the histograms of the pulse energies. ON pulses are about 40% weaker than OFF pulse. As the ON pulses is absorbed by atmospheric CH₄, the signal to noise ratio of the ON signal will be significantly lower than the OFF signal resulting in non-optimized DIAL measurement. To mitigate this, the Q-switch AOM is not completely turned off at the OFF pulse emission. The resulting lower gain entails lower OFF pulse energy. In addition, the remaining crystal gain increases the ON pulse energy. Therefore, by implementing non-symmetric operation of the Q-switch AOM, equal pulse energies can be obtained, as shown in the bottom graph of Fig. 5. As the gain is equal at every pulse emission, the energy stability is even better with an energy standard deviation 4 times lower.

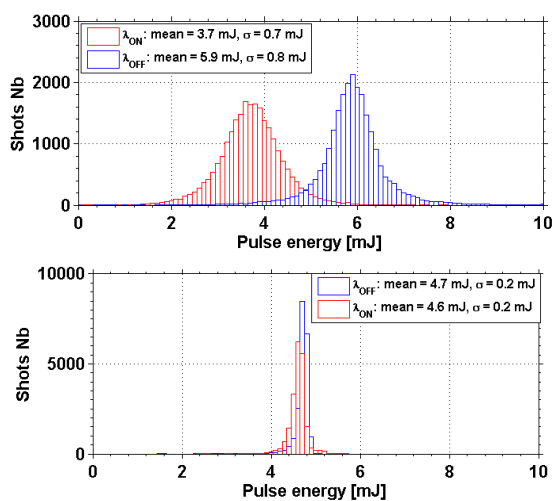


Figure 5. Histogram of the pulse energies with symmetric (top) and asymmetric (bottom) operation of the Q-switch AOM. PRF = 2kHz, Pump power = 60 W

To study the quality of the injection-seeding laser operation, the statistics of the beat notes frequencies between the pulse and the seeder are computed. The histograms of the beat note frequency for ON and OFF pulses are displayed in Fig. 6 at 2 kHz PRF and 60 W pump power.

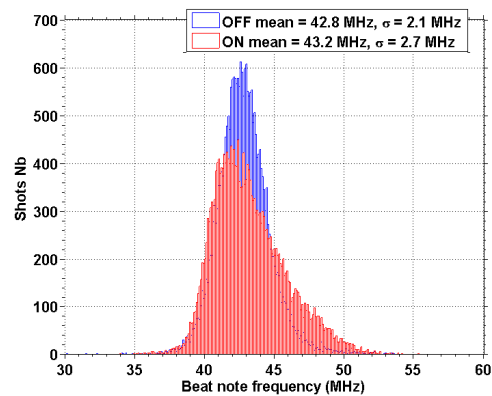


Figure 6. Histogram of the beat note frequency between the output pulse and the seeder. Asymmetric Q-switch AOM operation, PRF = 2 kHz, pump power = 60 W.

The ON and OFF pulses are generated with an asymmetric Q-switch AOM operation to obtain equal pulse energies. As the seeder is frequency shifted by the Q-switch AOM, the beat note frequency is close to the 41 MHz RF frequency applied to the AOM. The shot to shot standard deviations of the frequency jitter due to both the injection seeding process and the DFB bandwidth (1 MHz) are respectively 2.1 MHz and 2.7 MHz for OFF and ON pulses. The shape of the ON pulses frequency histogram is slightly asymmetric but the seeding process remains very efficient.

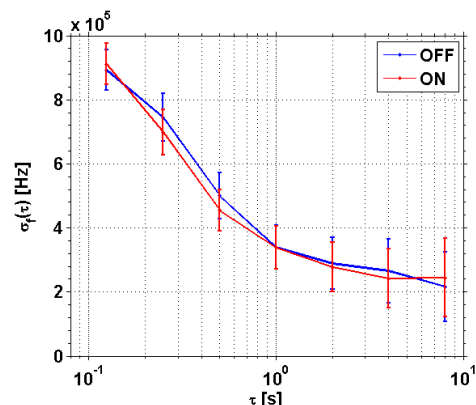


Figure 7. Allan deviation of the ON and OFF pulse frequencies

The frequency stability can be assessed using the Allan deviation as shown in Fig. 7. Both Allan deviation of the frequency decrease to

about 250 kHz for a few seconds integration time.

To assess the spectral purity of the laser a spectrum of a beat note between the seeder and the laser pulse is shown in Figure 8. The main frequency of the beat note corresponds to the mixing of the main cavity mode with the seeder around the AOM RF wave. The thin peak at 270 MHz results from the mixing of residual unseeded modes. This frequency is the free spectral range of the 1.1 m long cavity. The two broader peaks around the 270 MHz are from the mixing of the seeder with adjacent modes of the main seeded mode. They are broader because the seeder spectral width is larger than the non-seeded pulse spectral width. These unseeded adjacent modes are approximately 35 dB lower than the main seeded mode. This gives a spectral purity estimate larger than 99.93 %.

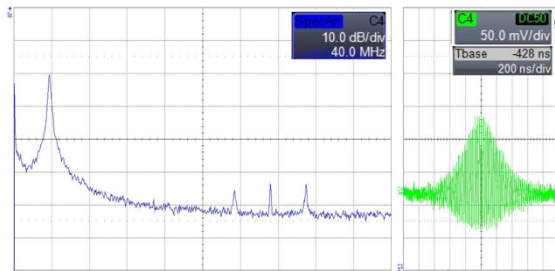


Figure 8. Oscilloscope capture of the beat note spectrum. Scale: 40 MHz/10 dB

The spectral drift of the ON seeder wavelength, locked to the cavity mode, has been monitored using a wavemeter. The drift was measured to be less than 40 MHz over few hours close to the accuracy of the wavemeter. The measurement was carried out in the lab with a stable ambient temperature. Other measurements will be carried out with a drift of the ambient temperature over several degrees to assess the thermal stability of the laser.

4. Conclusion

A dual wavelength laser emitter dedicated to DIAL measurements of atmospheric methane profiles has been developed and tested. An hybrid structure using a fiber pump laser and an Er:YAG cavity was used. It can deliver 8 mJ/1 kHz/300 ns or 4 mJ/2 kHz/ 575 ns pulses around the methane triplet line at 1645.55 nm (ON) and at 1645.3 nm (OFF). Despite the difference in emission cross section between the two wavelengths that required in other works to use several intra-cavity etalons, emission of equal pulse energies was demonstrated without etalon

through the asymmetric operation of the Q-switch AOM. The shot to shot standard deviation of the pulse frequency relative to the seeder is around 2.5 MHz for both wavelengths. The frequency Allan deviation reaches 250 kHz for a few seconds integration time. The difference between the seeded mode and unseeded modes is 35 dB showing a 99.97% spectral purity. All these results show that the laser emitter is relevant for precise and accurate CH₄ DIAL measurement. The full lidar system test including the hybrid Er:YAG laser is on the way.

5. References

- [1] Ehret, G.; Bousquet, P.; Pierangelo, C.; Alpers, M.; Millet, B.; Abshire, J.B.; Bovensmann, H.; Burrows, J.P.; Chevallier, F.; Ciais, P.; et al. "MERLIN: A French-German Space Lidar Mission Dedicated to Atmospheric Methane". *Remote Sens.* 2017, 9, 1052. doi:10.3390/rs9101052
- [2] H. Riris, K. Numata, S. Wu, B. Gonzalez, M. Rodriguez, S. Scott, S. Kawa and J. Mao, "Methane optical density measurements with an integrated path differential absorption lidar from an airborne platform", *J. Appl. Remote Sens.*, 11(3), 034001, (2017)
- [3] P. Tang, J. Liu, B. Huang, C. Xu, C. Zhao, and S. Wen, "Stable and wavelength-locked Q-switched narrow-linewidth Er:YAG laser at 1645 nm", *Opt. Express*, 23 (9) 11037, (2015)
- [4] Wang X., H. Fritsche, O. Lux, H.J. Eicher, Z.G. Zhao, C. Schuett and B. Kruschke, "Dual-wavelength Q-switched Er:YAG laser around 1.6 μm for methane differential absorption lidar", *Laser Phys. Lett.* **10**, 115804, (2013)
- [5] A. Aubourg, F. Balembois, P. Georges, "Comment on 'Dual wavelength Q-switched Er:YAG laser around 1.6 μm for methane differential absorption lidar'", *Laser Physics Lett.* **11**(4), 048001, (2014)
- [6] F. Gibert, D. Edouart, C. Cénac and F. Le Mounier, "2-μm high-power multiple-frequency Ho:YLF laser for DIAL application", *Appl. Phys. B*, doi : 10.1007/s00340-014-5784-3, 2014
- [7] Y. Shi, C. Gao, S. Wang, S. Li, R. Song, M. Zhang, M. Gao and Q. Wang, "High-energy, single-frequency, Q-switched Er:YAG laser with a double-crystals end-pumping architecture", *Opt. Express*, 27 (3), 2671-2680, (2019)